Title

Parieto-frontal network in humans studied by cortico-cortical evoked potential

Riki Matsumoto[1,2], Dileep.R.Nair[1], Akio Ikeda[2], Tomoyuki Fumuro[2], Eric Lapresto[1], Nobuhiro Mikuni[3,7], William Bingaman[1], Susumu Miyamoto[3], Hidenao Fukuyama[4], RyosukeTakahashi[2], Imad Najm[1], Hiroshi Shibasaki[2,5], Hans O. Lüders[6]

Epilepsy Center[1], Neurological institute, Cleveland Clinic, Cleveland, Ohio

Departments of Neurology[2] and Neurosurgery[3], Human Brain Research Center[4], Kyoto University Graduate School of Medicine, Kyoto, Japan

Department of Neurology[5], Takeda General Hospital, Kyoto, Japan

Epilepsy Center[6], University Hospitals Case Medical Center, Cleveland, Ohio

Department of Neurosurgery[7], Sapporo Medical University

Address correspondence to

Riki Matsumoto M.D., Ph.D.

Department of Neurology, Kyoto University Graduate School of Medicine

54 Kawahara-cho, Shogoin, Sakyo, Kyoto, JAPAN 606-8507

Tel: +81-75-751-3772, Fax: +81-75-751-9416

Email: matsumot@kuhp.kyoto-u.ac.jp

Running title: Parieto-frontal network studied by CCEP

Abstract

Parieto−frontal network is essential for sensorimotor integration in various complex behaviors, and its disruption is associated with pathophysiology of apraxia and visuo-spatial disorders. Despite advances in knowledge regarding specialized cortical areas for various sensorimotor transformations, little is known about the underlying cortico-cortical connectivity in humans. We investigated inter-areal connections of the lateral parieto−frontal network *in vivo* by means of cortico-cortical evoked potentials (CCEPs). Six patients with epilepsy and one with brain tumor were studied. With the use of subdural electrodes implanted for presurgical evaluation, network configuration was investigated by tracking the connections from the parietal stimulus site to the frontal site where the maximum CCEP was recorded. It was characterized by i) a near-to-near and distant-to-distant, mirror symmetric configuration across the central sulcus, ii) preserved dorso-ventral organization (the inferior parietal lobule to the ventral premotor area and the superior parietal lobule to the dorsal premotor area) and iii) projections to more than one frontal cortical sites in 56% of explored connections. These findings were also confirmed by the standardized parieto-frontal CCEP connectivity map constructed in reference to the Jülich cytoarchitectonic atlas in the MNI standard space. The present CCEP study provided an anatomical blueprint underlying the lateral parieto-frontal network and demonstrated a connectivity pattern similar to non-human primates in the newly developed inferior parietal lobule in humans.

Key words:

apraxia, cortico-cortical evoked potential, epilepsy, parieto-frontal network, functional connectivity, praxis movement

Abbreviations:

AD = afterdischarge; AIP = anterior intraparietal area; BA = Brodmann's area; CCEP = cortico-cortical evoked potential; DCR = direct cortical response; ECoG = electrocorticogram; FCD = focal cortical dysplasia; IFS = inferior frontal sulcus; IPS = intraparietal sulcus; IPL = inferior parietal lobule; MI = primary motor cortex; MIP = medial intraparietal ara; PM = lateral premotor cortex; PMd = dorsal premotor cortex; PMv = ventral premotor cortex; PPC = posterior parietal cortex; SFS = superior frontal sulcus; SI = primary somatosensory cortex; SPL = superior parietal lobule; SLF = superior longitudinal fasciculus; PE, PEc, PEip, PF, PFG, PGm of the macaque brain, according to Pandya and Seltzer (1982); 5M, 5L, 7PC, 7A, 7P, hIP1-3, OP1-4, PF, PFcm, PFm, PFt, PFop, PGa, PGp of the human brain, according to Caspers et al. (2008), Eickhoff et al. (2006) and Scheperjans et al. (2008)

Introduction

Parieto-frontal network is essential for sensorimotor integration in various complex behaviors, and its disruption is associated with pathophysiology of apraxia. Apraxia comprises a wide spectrum of impairment of skilled, learned movements that result from acquired brain diseases. It was a landmark proposal by Hugo Liepmann and Norman Geschwind when they posited that apraxia occurred as a result of disconnection of anatomically separate cortical regions (Liepmann, 1920; Geschwind 1965a,b). This concept was further developed by Damasio, Mesulam and colleagues (Geschwind and Damasio 1985; Mesulam 2000), in which the contemporary neuroanatomical framework underlying apraxia involved the parieto-frontal network connecting multiple specialized cortical areas. These areas were further grouped into territories which were thought to be connected through parallel, bidirectional pathways (see Catani and ffytche 2005; Leiguarda and Marsden 2000 for review). In monkeys, multiple parallel parieto-frontal circuits engaged in specific sensorimotor transformations have been described (Rizzolatti, et al. 1998); for example, visual and somatosensory transformations for reaching [MIP-F2]; transformation about the location of body parts necessary for the control of movements [PE-F1]; visuomotor transformation for grasping [AIP-F5]; and internal representation of action [PF-F5]. It has been hypothesized that unimodal apraxia such as optic ataxia (Balint 1909) and tactile apraxia (Binkofski, et al. 2001) is due to impairment of modality-selective sensorimotor transformation, while supramodal apraxia such as ideational and ideomotor apraxia is due to impairment of supra-modal sensory integration (Freund 2001) .

Lesion studies and functional activation studies have provided evidence for such a modular organization in the cortex (see Leiguarda and Marsden 2000; Freund 2001; Wheaton and Hallett 2007 for review). These studies also revealed functional lateralization of the parieto-frontal network: left hemisphere dominance for supramodal ideational and ideomotor apraxia and right hemisphere dominance for impairment of spatial awareness or hemispatial neglect (Corbetta and Shulman 2002). In contrast, anatomical knowledge of connecting pathways has, until recently, relied on tracer studies in non-human primates (Mesulam 2005). However, the development of a higher-order association area in the human parietal lobe, especially the inferior parietal lobule (IPL: Brodmann's area (BA) 39 and 40), made it difficult, if not impossible, to directly extrapolate the connectivity findings obtained in non-human primates (Brodmann 1905; Eidelberg and Galaburda 1984; Grefkes and Fink 2005; Van Essen, et al. 2001).

In vivo connectivity studies in humans have only recently begun using non-invasive methods, diffusion tractography in particular (Behrens, et al. 2003; Catani, et al. 2002; Wakana, et al. 2004). With the development of new algorithms such as multifiber probabilistic diffusion tractography, investigation of detailed cortico-cortical pathways, not only limited to the dense white mater bundles, has just begun (Tomassini, et al. 2007). These pathways, however, are solely determined by mathematical calculation of anisotropy of water molecules. Thus, further work is needed to understand the anatomical organization of the parieto-frontal network by means of different modalities. We have recently developed an *in vivo* electrical tract tracing method to study cortico-cortical

connections in humans [cortico-cortical evoked potential (CCEP)] (Matsumoto, et al. 2004a, 2004b, 2007a). By means of subdural electrodes implanted for presurgical evaluation of patients with intractable partial epilepsy or brain tumor, electrical pulses were applied directly to the cortex, and evoked cortical potentials were recorded from remote cortical regions. This technique provides a unique opportunity to electrophysiologically track functional connectivity among different cortical regions. In this study, we investigated the lateral parieto-frontal network underlying execution of praxis movements and its disturbance, apraxia by means of CCEP. We also attempted to provide a standardized connectivity map in reference to the Jülich cytoarchitectonic atlas by coregistering CCEP connectivity findings obtained upon individual basis into the Montreal Neurological Institute (MNI) standard space.

Material and Methods

Subjects

Seven patients, six with partial epilepsy and one with brain tumor, who underwent chronic subdural electrode placement covering the lateral fronto-parietal area for the presurgical evaluation, were studied (Table 1). In Patient 1-3, the epileptic foci were outside the lateral fronto-parietal area. Patient 4 had astrocytoma in the middle third of the left precentral gyrus. Patient 5-7 had the epileptic foci in the lateral fronto-parietal area: in the superior frontal gyrus (dysembryoplastic neuroepithelial tumor, Patient 5), the basal temporal region and the posterior part of the lateral temporo-parietal region (Patient 6), and the frontal operculum (Patient 7). Neurological examination was unremarkable

except Patient 4 who showed mild weakness of the right hand and dysarthria. The implanted electrodes were made of platinum, measuring 3.97 mm (Cleveland Clinic, Cleveland, OH) (Patient 1-3) or 2.3 mm (Ad-Tech, Rachine, WI) (Patient 4-7) in diameter with a center-to-center interelectrode distance of 1 cm. As a part of the routine presurgical evaluation, high frequency (50 Hz) electrical stimulation was performed for the purpose of functional cortical mapping (Lüders, et al. 1987). Cortical regions for electrical stimulation were determined solely for clinical purposes, and cortical mapping of the perirolandic area was performed in Patient 1 and 4-7. Normal configuration of the sensorimotor cortices was observed except for Patient 4 in whom the sensorimotor area was spilt by the tumor in the precentral gyrus. To define the precise location of each electrode on the surface of the brain, subdural electrodes were co-registered to three-dimensional volume-rendered MRIs, which were reconstructed from MPRAGE (Patient 1-3, 5-7) or FSPGR (Patient 4) sequences (1.5 T) performed after grid implantation. The location of each electrode was identified on the 2D MRIs using its signal void due to the property of the platinum alloy. Details of the methodology have been described elsewhere (Matsumoto, et al. 2003, 2004b). Major sulci in the lateral convexity were identified using the atlas of the cerebral sulci by Ono et al. (1990) as a reference.

The present study was approved by the Institutional Review Board Committee at Cleveland Clinic (IRB No. 4513) and by the Ethics Committee of Kyoto University Graduate School of Medicine (No. 443). Informed consent was obtained from all patients. Patient 2, 3, 5 and 7 have been reported elsewhere for entirely different purposes (Ikeda, et al. 2009; Matsumoto, et al. 2004b,

2007a, 2011)

[Table 1 Patient profile]

Stimulus condition and data acquisition of CCEP

Details of the CCEP methodology have been described elsewhere (Matsumoto, et al. 2004a, 2004b, 2007a). In brief, electrical stimulation was applied in a bipolar manner to a pair of adjacently placed subdural electrodes by a constant-current stimulator (Grass S88, Astro-Med, Inc., RI, or Electrical Stimulator SEN-7203, Nihon Kohden, Tokyo, Japan). The electrical stimulus consisted of a square wave pulse of 0.3 ms duration, which was given at a fixed frequency of 1 Hz in alternating polarity. The stimulus strength was 80–100% of the intensity that produced either clinical signs or afterdischarges (ADs) upon 50 Hz stimulation. If no clinical signs or ADs were elicited at 15 mA, the intensity was set at 12–15 mA. In the cortical areas where 50 Hz stimulation was not performed for clinical purposes, the current intensity was set at 12-15 mA after confirming the absence of ADs at 1 Hz stimulation frequency. In cases in which excessive artifacts obscured the evoked potential recordings, the intensity was lowered stepwise by 1 mA until artifacts became small enough to visualize the evoked responses.

Electrocorticograms (ECoGs) were recorded with a bandpass filter of 1–1000 Hz and a sampling rate of 2500 Hz in Patient 1-3 (Axon Epoch 2000 Neurological Workstation, Axon Systems Inc., NY), with the filter of 0.5–1500 Hz at a sampling rate of 5000 Hz in Patient 4 and 5 (Biotop, NEC-Sanei, Tokyo, Japan), and with the filter of 0.08–300/600 Hz at a sampling rate or 1000/2000

Hz in Patient 6 and 7 (EEG-1100, Nihon Kohden, Tokyo, Japan). Recordings from subdural electrodes were referenced to a scalp electrode placed on the skin over the mastoid process contralateral to the side of electrode implantation. CCEPs were obtained by averaging ECoGs with a time window of 200 ms, time-locked to the stimulus onset. In each session, at least two trials of 20–100 responses each were averaged separately to confirm the reproducibility of the responses. During the recording of CCEPs, the patients were requested not to perform any specific task. They were typically lying or sitting on the bed.

Electrode pairs in the lateral parietal area were stimulated and CCEPs were recorded from the lateral convexity of the frontal lobe. Four to 14 pairs of adjacent electrodes were stimulated per patient, amounting to 64 pairs in total (Table 1). Stimulation was performed in the postcentral gyrus (i.e., primary somatosensory cortex (SI)) at 18 stimulus sites and in the parietal area caudal to the postcentral sulcus (i.e., posterior parietal cortex (PPC)) at 46 stimulus sites. CCEPs were recorded from subdural electrodes (11-23 electrodes per patient) placed on the lateral premotor (PM) and primary motor (MI) cortices (Table 1). Since the extent of coverage by subdural electrodes was determined solely by clinical needs, the grids mainly covered the ventral half of the lateral parieto-frontal area in Patient 2, 6, 7, and the dorsal half in Patient 5, while the other patients had coverage over both the dorsal and ventral regions. Possible reciprocal connections from the frontal cortex to the parietal cortex were not investigated in this study, because of the limited time allowed for the clinical study. The reciprocal connections seem to be a general rule in humans according to our previous CCEP studies on cortical motor and language

networks (Matsumoto, et al. 2004b, 2007a).

CCEP analysis

In the previous CCEP study on the language system (Matsumoto, et al. 2004b), the CCEP consisted of an early (N1) and a late (N2) negative potential. In this study, we focused on the analysis of the N1 potential since not all the responses showed a clear N2 peak. The N1 peak was visually identified as the first negative deflection that was clearly distinguishable from the stimulus artifact. The N1 amplitude was measured as reported elsewhere (Matsumoto, et al. 2004b). In brief, the amplitude was measured from the line connecting the preceding and following troughs to the N1 peak. This way of measurement was employed because the conventional trough-to-peak measurement was difficult due to the preceding stimulus artifact in some records.

The parieto-frontal connections from the site of stimulation were traced according to the distribution of the CCEP field. The predominant connection was defined based on the most prominent CCEP field with the maximum N1 response. Besides the most prominent field, if any other field with a discrete N1 potential was spatially separated from the main field, that field was considered as a separate CCEP field, indicating multiple divergent connections.

To investigate the anatomical relationship between the site of stimulation and that of the maximum response, these sites from each patient were plotted on common coordinates. The stimulus site was defined as the midpoint of the pair of stimulating electrodes, and the site of the maximum response as the center of the electrode showing the maximum N1 potential (Fig. 1). For both the

parietal stimulus sites and the frontal recording sites, the relationship was displayed in the rostro-caudal dimension (Fig. 1A) as well as in the dorso-ventral dimension (Fig. 1B). For the rostro-caudal dimension, the surface distance of the cortical sites from the central sulcus was displayed. To better describe the functional property in the dorso-ventral dimension, the distance of the parietal stimulus sites was measured from the border between superior (SPL) and inferior (IPL) parietal lobules, namely intraparietal sulcus (IPS), and the distance of the frontal recording sites was measured from the border between the dorsal (PMd) and ventral (PMv) premotor areas. Because the functional motor mapping was not performed in all the patients and no macroscopic anatomical landmark existed to locate the border between PMd and PMv (Geyer, et al. 2000; Picard and Strick 2001; Rizzolatti, et al. 1998), the virtual border was set arbitrarily as the line parallel to the AC-PC line crossing the midpoint between the caudal ends of the superior (SFS) and inferior (IFS) frontal sulci. When the stimulus and response sites were situated, respectively, on the post- and pre-central gyri, the distance was calculated from the extrapolated border drawn from the above-described borderline toward the central sulcus.

[Figure 1 inserted here]

Standardization of the connectivity findings obtained by CCEP

In order to better delineate the anatomical localization of the parietal stimulus and frontal response sites in the MNI standard space, electrodes identified on the T1 volume acquisition (MPRAGE or FSPGR) taken after grid implantation were non-linearly co-registered to the T1 volume acquisition taken before

implantation, then to the MNI standard space (ICBM-152) using FNIRT of the FSL software (www.fmrib.ox.ac.uk/fsl/fnirt/). This method has been reported elsewhere for standardization of the electrode locations (Matsumoto, et al. 2011). Anatomical parcellation of the parietal stimulus site was identified in reference to the location of the midpoint of the pair of stimulating electrodes in the cytoarchitectonic probabilistic map of the Jülich histological atlas (Caspers, et al. 2008; Eickhoff, et al. 2006a; Scheperjans, et al. 2008). The parietal label having the highest probability was taken as the label of the stimulus site using Eickhoff's anatomy toolbox v1.5 incorporated in FSLView (www.fmrib.ox.ac.uk/fsl/fslview/) (Eickhoff, et al. 2006b). The label was chosen from the parietal labels on the lateral convexity: BA1, BA2, 5M, 5L, 7PC, 7A, 7P, hIP1-3, OP1-4, PF, PFcm, PFm, PFt, PFop, PGa, PGp. When the MNI coordinate of the stimulus site did not provide any probability of the cortical labels, i.e., the coordinate was on or slightly above the surface of the MNI standard brain, the location of the coordinate was shifted perpendicular toward the cortical surface (<5 mm) until the good probability was obtained in the probabilistic map. Regarding the frontal CCEP responses, the location of the electrode showing the maximum response, i.e., the target site of the predominant connection from the stimulus site, was identified in the same manner. If there were additional, separate CCEP fields, the electrode showing the maximum response of each additional field, i.e., the target site of the additional divergent connection from the stimulus site, was also identified. Because of our interest in parcellation along the dorsoventral axis, BA1, BA2 and BA6 were further divided into their dorsal and ventral subdivisions (e.g., BA1d, BA1v). The border between the dorsal and ventral subdivisions was

set at z = 48 according to the recent parcellation of the premotor areas by probabilistic diffusion tractography (Tomassini, et al. 2007). BA6 was further divided into its rostral (BA6dr) and caudal subdivisions (BA6dc, BA6vc) in reference to the precentral sulcus (Matsumoto, et al. 2003, 2007a; Picard and Strick 2001). Since cytoarchitechtonic parcellation was not completed in the frontal lobe in the Jülich histological atlas, we defined the dorsal half of the most caudal part of the middle frontal gyrus as BA6dr (the dorso-rostral division of the premotor area). Accordingly, the frontal labels on the crown part of the lateral convexity were categorized into BA6dr, BA6dc, BA6vc, BA44, and BA45. Because BA44 was situated immediately rostral to the inferior precentral suclus, BA44 and 45 were regarded as the rostral part of PMv in this study.

For the 3D display purpose, the baview software (Yamamoto, et al. 2011) was used to show the 3D view of the predominant and additional connections (i.e., stimulus and response sites) in the fsaverage brain that is constructed compatible to the initial MNI template (MNI305) in the FreeSurfer software (http://surfer.nmr.mgh.harvard.edu/).

Results

Analysis of the parieto-frontal network in the individual space

In all the patients investigated, stimulation of the parietal lobe elicited CCEPs in the frontal lobe. CCEPs were recognized in a total of 52 out of 64 stimulus sites (81%, 2-14 sites per patient). As shown in a representative case (Fig. 2), the majority of CCEPs consisted of a surface negative potential (N1), and when the stimulus artifact was relatively small, a preceding small positive deflection could

be recognized. The predominant parieto-frontal connections from the stimulus sites were determined based on the maximum N1 response. In terms of the CCEP distribution along the rostro-caudal dimension, stimulation of the postcentral gyrus (18 sites across all subjects) elicited the largest N1 almost exclusively in the precentral gyrus (14 sites; see Fig. 2C, 2F for example) and rarely in PM rostral to the precentral sulcus (2 site). In contrast, upon stimulation of PPC (46 sites), the majority of CCEPs were observed in PM rostral to the precentral sulcus (32 sites; Fig. 2A, D, E), and only a few responses were seen maximum in the precentral gyrus (4 sites; Fig. 2B). This near-to-near and distant-to-distant, mirror-symmetric configuration across the central sulcus was substantiated in the regression analysis (Fig. 3A). In terms of the distance from the central sulcus along the rostro-caudal dimension, a positive correlation was observed between the sites of stimulation and maximum response ($R = 0.791$, $p < 0.0001$). Namely, as the parietal stimulus site was more distant from the central sulcus, the maximum response recorded from the frontal area was more distant from the central sulcus. This mirror-symmetric configuration was further supported by a significant positive correlation between the N1 peak latency and the surface distance from the parietal stimulus sites to the frontal recording sites (Fig. 3C, $R = 0.683$, $p < 0.0001$); the N1 latency was longer in proportion to the distance between the parietal stimulus sites and frontal recording sites. Regarding the network configuration in the dorso-ventral dimension, the regression analysis showed a significant correlation between the parietal stimulus sites and the frontal recording sites in terms of the distance from the dorso-ventral border in the same direction (either ventral or dorsal) (Fig. 3B, R =

0.758, $p < 0.0001$). The more dorsal parietal stimulation resulted in the more dorsal frontal response, and vice versa. In other words, the dorso-ventral configuration (i.e., dorsal parietal to dorsal frontal and ventral parietal to ventral frontal areas) was preserved across the central sulcus.

Besides the predominant parieto-frontal connections as judged by the maximum CCEP response, additional frontal CCEP fields were identified in 29 out of 52 (56%) stimulus sites that elicited CCEPs upon stimulation (Fig. 2A-E, Fig. 4). In 13 out of the 29 stimulus sites (25% of total), three (12 sites) or four (1) independent fields were identified in the lateral frontal area (see Fig. 2A, B, Fig 4).

In Patient 4 who had a tumor in the precentral gyrus, a ventral parieto-frontal connection was preserved in the vicinity of the tumor (Fig. 5). Stimulation of the supramarginal gyrus elicited a maximum response at PMv (supramarginal gyrus - PMv circuit). The circuit configuration was similar to those found in other epilepsy patients (e.g., Fig 2E). In none of the patients, seizures were provoked by single pulse stimulation of the lateral parietal area.

[Figure 2-5 inserted here, please make Fig. 2 in a large size (using the whole width of the page) so that the readers can see the minute and thin waveforms]

Analysis of the parieto-frontal network in the standardized space

The locations of the parietal stimulus and frontal response sites in the MNI standard space were labeled according to the Jülich cytoarchitectonic atlas (Table 2). Cortical regions located within the sulcal part of the parietal lobe (e.g.,

PFcm, hIP 1-3, OP1-3) were not identified as the most probable label. Stimulation of the postcentral gyrus (BA1, BA2) almost exclusively elicited the maximum CCEP responses in the precentral gyrus (at BA6dc, 6vc in 15/17 stimulus sites) with the preserved dorso-ventral organization, i.e., from BA1v&2v to the ventral frontal areas, and from BA1d&2d to the dorsal frontal areas. In the inferior parietal lobule (30 stimulus sites), predominant connections were observed from the angular gyrus [PGa (3), PGp (3)] mostly to BA44 (3) and BA6dr (2); from the supramarginal gyrus [PFop (1), PFt (1), PF (12), PFm (7)] to BA44 (11), BA6dr (4), BA45 (3) and caudal BA6 (BA6dc, 6vc) (3); and from the parietal operculum [OP4 (3)] to BA6vc (2) and BA44 (1). The superior parietal lobule [7PC (2), 7A (3)] connected with BA6dr (2), caudal BA6 (2) and BA44 (1). Results of the additional connections revealed by additional, separate CCEP fields are also summarized in Table 2. The parietal stimulus and frontal response sites from all the subjects (Patient 1-7) are displayed together in the MNI standard space (Fig. 6). The two major configurations of the parieto-frontal network – mirror symmetry across the central sulcus and preserved dorso-ventral organization – were also confirmed in this 3D view. The MNI coordinates and cytoarchitectonic labels of the parietal stimulus and frontal response sites are available for all the patients investigated in the present study in Table 3.

[Figure 6 and Table 2 inserted here, please make Fig. 6 in a large size (using the whole width of the page) so that the readers can recognize each small points on the 3D brain]

[Please insert Table 3 here using the whole width of the page]

Discussion

In this study, we were able to map a global topographical geometry of the lateral parieto-frontal network. It was characterized by: i) mirror symmetry across the central sulcus (the more caudal the parietal stimulus site, the more rostral the frontal response site, and vice versa), ii) preserved dorso-ventral organization of the predominant circuits (dorsal parietal to dorsal frontal and ventral parietal to ventral frontal areas), and iii) projections to more than one frontal cortical sites (predominant and additional circuits) in 56% of the explored connections. By incorporating CCEP connectivity findings into the MNI standard space, we were able to clarify the anatomical parcellation of the parietal stimulus and frontal response sites in reference to the Jülich cytoarchitectonic atlas. The modes of connectivity are discussed in the context of the functional organization of the parieto-frontal circuits in special relation to apraxia.

Implication and limitation of CCEP

Knowledge of cortico-cortical connections in humans has been limited until very recently because of the paucity of the available *in vivo* techniques in humans (Mesulam 2005). The CCEP technique provides a unique opportunity to electrophysiologically track cortico-cortical connections *in vivo* by stimulating a part of the cortex through subdural or depth electrodes and recording evoked cortical potentials that emanate from the remote cortical regions. This method has been successfully applied to delineate cortico-cortical networks involved in

language and motor systems (Matsumoto, et al. 2004b, 2007a) as well as subcortico-cortical networks (Lacruz, et al. 2007; Rosenberg, et al. 2009) . In contrast to diffusion tractography that is calculated solely by mathematical calculation of anisotropy of water molecules, the CCEP technique has an advantage of tracking the inter-areal connectivity physiologically, providing directional as well as temporal information. In this regard CCEP may well be regarded as 'functional tractography' as compared with 'anatomical fiber tractography' visualized by diffusion tractography. By means of precise electrode localization in relation to individual sulci on 3D MRI, the functional tractography allows delineation of cortico-cortical connectivity with spatial resolution of 1 cm. However, as the stimulation and recording was performed by subdural electrodes, the investigation was limited to the cortical surface, i.e., the crown part, and little information was available about the sulcal part such as IPS. Furthermore, this technique cannot identify the underlying anatomical pathways between the stimulus and response sites.

The precise generator mechanisms of CCEP still remain unknown. The possible mechanisms have been extensively discussed elsewhere (Matsumoto and Nair 2007; Matsumoto, et al. 2004b, 2007a). In brief, we speculate that, upon cortical stimulation, orthodromic excitation of cortico-cortical projection neurons occurs through direct depolarization of the initial segment as well as synaptic excitation in the local circuit. The latter is mainly mediated by ascending recurrent axon collaterals of the pyramidal neurons and partly by excitatory interneurons. With "oligo-synaptic" excitation of the cortico-cortical projection neurons, the impulse travels through cortico-cortical projection fibers to the

target cortex with some jitter, and then generates a relatively blunt N1 potential. Indeed, a similar blunt cortical potential called ‘direct cortical response (DCR)’ was recorded in the immediately adjacent cortex upon local cortical stimulation in animals and humans (Adrian 1936; Goldring, et al. 1994). Of note, DCR shares the morphology and latency (~10 ms in humans) with the CCEP recorded from the very adjacent cortex to the stimulus site. Animal experiments have shown that DCR is oligosynaptic and local in origin since it is observed in completely isolated cortex (Jerva, et al. 1960; Li and Chou 1962). The present findings provided some insight into the underlying anatomical pathway between the stimulus and target cortices. The linear correlation between the N1 peak latency and the surface distance from the parietal stimulus site to the frontal response site (Fig. 3C) favors the direct cortico-cortical white matter pathway, because, as the surface distance is longer, the actual white matter pathway connecting the two cortical sites and accordingly its traveling time is expected to be proportionally longer. By contrast, this would not be the case for the indirect cortico-subcortico-cortical pathways. Since the distance between the cortical surface and the subcortical structures such as thalamus may not significantly differ depending on the location of the stimulus or response sites, the latency of CCEP may fail to correlate with the surface distance between the two cortical sites in that case.

Blueprint of the human lateral parieto-frontal network

By means of direct electrical cortical stimulation, the present CCEP study provided blueprint of the lateral parieto-frontal network in humans. Based upon

the predominant circuits revealed by the maximum CCEP response, the dorso-ventral configuration was preserved across the central sulcus (i.e., dorsal parietal to dorsal frontal area, and vice versa). This relationship is consistent with the known organization of the lateral parieto-frontal circuits in monkeys: strong inputs from the superior parietal areas (MIP, PEip, posterior SPL, medial SPL, PEc, PGm and V6A) to PMd (Fang, et al. 2005; Johnson, et al. 1996; Matelli, et al. 1998; Schmahmann and Pandya 2006; Stepniewska, et al. 2006; Tanne, et al. 1995; Wise, et al. 1997) and from the inferior parietal areas (AIP, PF and PFG) to PMv (Cavada and Goldman-Rakic 1989; Lewis and Van Essen 2000; Luppino, et al. 1999; Matelli, et al. 1986; Rizzolatti, et al. 1998; Rozzi, et al. 2006; Schmahmann and Pandya 2006). The preserved dorso-ventral organization noted in the functional tractography study reported here complements the recent similar associations revealed by probabilistic diffusion tractography (Tomassini, et al. 2007). It serves as anatomical substrates for segregated parieto-frontal circuits revealed by fMRI activation studies: SPL-PMd circuit for reaching and arbitrary action selection (Astafiev, et al. 2003; Grol, et al. 2006; Prado, et al. 2005; Simon, et al. 2002), AIP-PMv for grasping and manual exploration of 3D objects (Binkofski, et al. 1999; Binkofski, et al. 1998; Decety, et al. 1994; Grafton, et al. 1996; Hattori, et al. 2009; Simon, et al. 2002), left IPL-PMv for tool-use planning and execution (Fridman, et al. 2006; Johnson-Frey, et al. 2005), and right IPL-PMv and the adjacent prefrontal cortex for spatial awareness (Corbetta and Shulman 2002). Furthermore, the present study demonstrated that the similar principle might be applied to the newly emerged inferior parietal regions in humans (BA 39 and 40; see Fig 2D-F, 4A, 6 for example), the key structures

for multimodal convergence essential for higher cognitive functions such as tool-use, language and calculation (Catani and ffytche 2005; Matsuhashi, et al. 2004). In fact, the ventral parieto-premotor network is also activated during calculation and language tasks (Dehaene, et al. 1999; Simon, et al. 2004; Vigneau, et al. 2006).

Regarding connectivity along the rostro-caudal axis, the present study showed predominant connections from SI to MI for final execution of limb movements as expected, and from PPC to PM for sensorimotor transformations. Furthermore, regression analysis of the distance from the central sulcus to the stimulus sites and to the recording sites revealed that the more caudal PPC connected to the more rostral PM and vice versa. This mirror-symmetric organization provides additional insights into the functional organization of the lateral parieto-frontal network. PM, being situated between the prefrontal area and MI, plays a role in mediating the transition from cognitive to motor functions, with the more rostral parts primarily related to sensory or cognitive aspects of motor behavior and the more caudal parts to the movement execution itself. Microelectrode recording in monkeys and subdural macroelectrode recording in humans have revealed that neurons possessing sensory properties are more frequently found in the rostral PM and those possessing motor properties more frequently in the caudal PM (Johnson, et al. 1996; Matsumoto, et al. 2003; Weinrich, et al. 1984). A corresponding but oppositely oriented gradient was observed in SPL in an instructed-delay reaching task in monkeys (Johnson, et al. 1996). Of note, in this task neurons of similar properties in PM and SPL were interconnected by cortico-cortical projections. Interestingly, a similar reverse of

functional gradient was observed in humans for tool-use gestures in the left hemisphere (Fridman, et al. 2006; Johnson-Frey, et al. 2005). In PPC, planning-related activation was located more caudal and ventral to that associated with execution, while in PMv the former was situated more rostrally to the latter. The mirror-symmetric configuration seems to be a general organizational framework in the lateral parieto-frontal network according to the fMRI analysis of various cognitive tasks using an automatized clustering algorithm (Simon, et al. 2004). A recent hypothesis of tension-based cortical folding may further support the mirror-symmetric organization, a principle that serves to minimize connection lengths in the brain (Van Essen 1997).

In order to further generalize the connectivity findings obtained by CCEPs in individual patients, we attempted to provide the standardized connectivity map by gathering the sites of stimulation and responses from all the patients in the present study, and by coregistering them into the MNI standard space (see Table 3 for individual MNI coordinates). By employing the Jülich cytoarchitectonic probabilistic map that is based on quantitative, observer independent definitions of cytoarchitectonic borders, we were able to integrate physiological CCEP findings with the state-of-art anatomical parcellation of the human parietal lobe. The present standardized connectivity map would help us delineate the segregation of information flow for specific functions and sensorimotor integration in the parieto-frontal network. In particular, by providing the origins and terminations of the parieto-frontal connections (see Table 2, 3 and Fig. 6), the present connectivity findings complement the recent segmentations of the superior longitudinal fasciculus (SLF) by means of diffusion

tractography (Makris, et al. 2005; Rushworth, et al. 2006). Based on the knowledge of SLF subcomponents (SLF I, II, III) as revealed by invasive tracer studies in the monkey brain (Petrides and Pandya 1984; Schmahmann and Pandya 2006), fiber pathways were tracked from the stem portion of each subcomponent that had characteristic orientation. SLF I was located in the white matter of the superior parietal and superior frontal areas and extended from the superior and medial parietal areas to the dorsal premotor and dorsolateral prefrontal areas. SLF II occupied the central core of the white matter above the insula and extended from the posterior IPL to the caudal–lateral prefrontal or premotor regions. SLF III was situated in the white matter of the parietal and frontal opercula and extended from the anterior IPL to the ventral premotor and prefrontal regions.

Several limitations should be noted to interpret the present connectivity findings. First, the extent of coverage by subdural electrodes was determined due to clinical needs by all means; SPL was less covered than IPL in the parietal lobe, and BA45 was less covered than BA44 in the frontal lobe. Second, the gender as well as hemispheric difference of the parieto-frontal network could not be evaluated due to the limited number of patients. Further case accumulation is needed to investigate these differences. Third, possible effects of the pathology on the network should be noted in patients having a brain tumor or epileptic focus in the lateral parieto-frontal area. This matter is discussed in the next section.

Clinical relevance

In the sequential control of actions, sensorimotor integration leading to action is mainly processed in the dorsal pathway (PPC and PM), while the pragmatic process of visual information about object attributes or object recognition occurs through the ventral pathway (occipito-temporal cortex) (Goodale and Milner 1992). Consequently, lesions of the ventral stream produce visual agnosia, while those of the dorsal stream (parieto-frontal circuits) give rise to deficits in sensorimotor transformation, namely, apraxia. Lesion studies show that a wide range of sensorimotor functions can be selectively disturbed in patients with parietal lobe damage. Lesions of the rostral and caudal SPL cause unimodal, somatosensorimotor-selective, tactile apraxia (Binkofski, et al. 2001) and visuomotor-selective, optic ataxia (Balint 1909; Battaglia-Mayer and Caminiti 2002; Karnath and Perenin 2005; Perenin and Vighetto 1988), respectively. Lesions involving the anterior lateral bank of IPS (human homologue of the anterior intraparietal area (AIP)) cause selective deficits in coordination of the finger movements required for grasping (Binkofski, et al. 1998). Lesions in IPL, IPS and partly SPL of the left hemisphere produced supramodal ideomotor apraxia (Haaland, et al. 2000; Halsband, et al. 2001; Heilman and Rothi 2003). Ideomotor apraxia is characterized by impairment of skilled actions that cannot be explained by lower-level perceptual or motor deficits (Leiguarda and Marsden 2000; Wheaton and Hallett 2007).

In contrast to discrete parietal lesions showing distinct apraxia, studies exploring possible clinical-anatomical correlations in the frontal lobe largely have failed to unveil a consistent and specific lesion site (Leiguarda and Marsden 2000). Only a few studies have clarified PM lesions responsible for ideomotor

(Faglioni and Basso 1985; Haaland, et al. 2000; Raymer, et al. 1999) and limb-kinetic (Kleist 1931; Luria 1980) apraxia. This is partly because lesions that involve the motor area projecting the corticospinal pathway (i.e., BA4 or caudal BA6) and Broca's area cause concomitant paresis and aphasia, respectively. Moreover, relative lack of selectivity of the frontal lesions for producing discrete apraxia could be ascribed to the divergent parieto-frontal connections as seen in 56% of the connections in the present CCEP study. The divergent connections would lead to 'cross-talk' with the predominant parieto-frontal connections. It could be argued that praxis movement is conducted by parallel anatomofunctional neuronal systems, each controlling specific processes, working in concert. The significance of the whole network in action generation is further supported by the fact that lesions not only in the cortex but also in the white matter in the left hemisphere could cause ideomotor apraxia (Papagno, et al. 1993). Moreover, increased cortico-cortical coherence of electroencephalogram (EEG) between the left PPC and PM was observed during preparation and execution of praxis movements (Wheaton, et al. 2005), indicating the importance of dynamic synchronization of the parieto-frontal network in action generation.

Significance of the parieto-frontal network is also appreciated for other higher cognitive functions, such as language and spatial awareness. The left ventral parieto-frontal connections observed between the supramarginal and the ventral frontal cortex (i.e., connections from PF/PFm in Fig. 6) have a striking similarity with the anterior segment of the arcuate fasciculus of Catani et al. (2005). Indeed, intraoperative electrical stimulation of the underlying subcortical

pathway as well as the ventral parieto-frontal cortices produced impairment of verbal fluency abilities (Duffau et al., 2003). While the language and praxis functions are largely lateralized to the left hemisphere, spatial awareness is the right-sided higher cognitive function involving the parieto-frontal network (Corbetta and Shulman 2002; Thiebaut de Schotten et al. 2011). Not only the lesions in the parieto-frontal cortex but also the lesions in SLF II and III are reported to produce hemispatial neglect (Doricchi, et al. 2008; Doricchi and Tomaiuolo 2003; He, et al. 2007). Furthermore, intraoperative electrical stimulation of SLF II produced transient hemispatial neglect, supporting the importance of the parieto-frontal connection in spatial awareness (Thiebaut de Schotten, et al. 2005).

In the present study, repetitive single pulse electrical stimulation was employed to map inter-areal connectivity. Single pulse stimulation is usually not intense enough to produce any deficits in higher brain functions. For future clinical application to map out the network for praxis movement and other higher cognitive functions, high frequency stimulation is needed to better delineate behavior impairment. It is expected to complement the present CCEP study by causing transient functional impairment of individual functions involved in the parieto-frontal network. Although the present investigation was limited to the patients undergoing invasive presurgical evaluation, a combined CCEP and diffusion tractography study in this patient population will provide a rare yet valuable opportunity to better understand the contemporary disconnection framework that highlights both specialization of the association cortices and connections between those brain regions (Catani and ffytche 2005). Recently

developed elaborate algorithms such as probabilistic diffusion tractography that incorporates multiple-fiber estimation will be of significant benefit for delineating subcortical pathways linking the stimulus and recording cortical sites (Behrens, et al. 2007). For elucidating roles of the medial parieto-frontal circuits as well as hemispheric difference of the parieto-frontal network related to praxis movements and other cognitive functions, a future combined study based on the accumulation of further cases is warranted.

It should be noted that the present study was carried out in patients with intractable partial epilepsy or brain tumor. While the parieto-frontal connectivity was studied in the presumably normal cortex away from the epileptic focus in Patient 1-3, Patient 5-7 had the foci within the lateral parieto-frontal area. While Patient 5 had dysembryoplastic neuroepithelial tumor 2 cm rostral to the precentral sulcus in the superior frontal gyrus, Patient 6 and 7 had normal MRI and the pathological diagnosis of focal cortical dysplasia (FCD) type 1A. Since 'MRI-negative' FCD are reported to have normal cortical functions and cortico-cortical connections (Marusic, et al. 2002; Matsumoto, et al. 2007a) and normal somatotopy was indeed observed in the sensorimotor strip upon high frequency electrical stimulation in all the three patients, these patients most likely had normal connectivity pattern in the parieto-frontal area. In Patient 4, the connectivity was investigated close to a perirolandic tumor. In this particular case, the CCEP investigation delineated a ventral parieto-frontal circuit preserved in the vicinity of the lesion with the same global geometry as observed in other patients (Fig. 5). Since CCEP studies are relatively easy to perform (each average from a given stimulus site takes only 1–2 m in and does not

require much of the patients' cooperation) and a chance of provoking seizures is extremely low (Matsumoto and Nair 2007), the CCEP technique could be applicable in an intraoperative setting to identify and monitor the functionally important network in the vicinity of lesions such as tumors. In the present study, we did not recruit epilepsy patients who had core epileptogenic areas in the lateral parietal area. It is through the parieto-frontal network that, in patients with parieto-occipital lobe epilepsy, epileptic discharges spread to the frontal lobe and manifest ictal semiology of frontal lobe epilepsy (Ajmone-Marsan and Ralston 1957; Ikeda, et al. 2002). By applying single pulse stimulation to the ictal onset zone, we could delineate cortico-cortical network involved in spike propagation in each individual patient (Matsumoto, et al. 2007b). This would be clinically useful to differentiate "green" spread spikes from "red" spikes originating from the epileptogenic focus.

Acknowledgments

We wish to thank Timothy O'Connor, Karl Horning, Mary Jo Sullivan, Pin Liu and Dr. Rei Enatsu for technical assistance. We are also grateful for Dr. Hiroki Yamamoto for his assistance in standardization of the CCEP connectivity findings. This work was supported by Cleveland Clinic (the Advanced International Clinical Fellowship Award to R.M.), the Japan Ministry of Education, Culture, Sports, Science and Technology (MEXT) (Grants-in-Aid for Scientific Research (C) 20591022 to R.M.) and the Japan Epilepsy Research Foundation (the Research Grant to R.M.).

Conflicts of Interests: None declared.

References

Adrian E. (1936): The spread of activity in the cerebral cortex. J Physiol (Lond) 88:127-61.

Ajmone-Marsan C, Ralston B. (1957): The Epileptic Seizure. Its Functional Morphology and Diagnostic Significance. Springfield: Charles C Thomas.

Astafiev SV, Shulman GL, Stanley CM, Snyder AZ, Van Essen DC, Corbetta M. (2003): Functional organization of human intraparietal and frontal cortex for attending, looking, and pointing. J Neurosci 23(11):4689-99.

Balint R. (1909): Seelenla¨hmung des Schauens, optische Ataxie,ra¨umliche Sto¨rung der Aufmerksamkeit. Monatsschr. Psychiatr. Neurol. 25:51-81.

Battaglia-Mayer A, Caminiti R. (2002): Optic ataxia as a result of the breakdown of the global tuning fields of parietal neurones. Brain 125(Pt 2):225-37.

Behrens TE, Berg HJ, Jbabdi S, Rushworth MF, Woolrich MW. (2007): Probabilistic diffusion tractography with multiple fibre orientations: What can we gain? Neuroimage 34(1):144-55.

Behrens TEJ, Woolrich MW, Jenkinson M, Johansen-Berg H, Nunes RG, Clare S, Matthews PM, Brady JM, Smith SM. (2003): Characterization and Propagation of Uncertainty in Diffusion-Weighted MR Imaging. Magnetic Resonance in Medicine 50(5):1077-1088.

Binkofski F, Buccino G, Posse S, Seitz RJ, Rizzolatti G, Freund H. (1999): A fronto-parietal circuit for object manipulation in man: evidence from an fMRI-study. Eur J Neurosci 11(9):3276-86.

Binkofski F, Dohle C, Posse S, Stephan KM, Hefter H, Seitz RJ, Freund HJ. (1998): Human anterior intraparietal area subserves prehension: a

combined lesion and functional MRI activation study. Neurology 50(5):1253-9.

Binkofski F, Kunesch E, Classen J, Seitz RJ, Freund HJ. (2001): Tactile apraxia: unimodal apractic disorder of tactile object exploration associated with parietal lobe lesions. Brain 124(Pt 1):132-44.

Brodmann K. (1905): Beitrage zu¨r histologischen localisation der grosshirnrinde, dritte mitteilung: die rinderfelder der niederen affen. J Psychol Neurol 4:177-226.

Caspers S, Eickhoff SB, Geyer S, Scheperjans F, Mohlberg H, Zilles K, Amunts K. (2008): The human inferior parietal lobule in stereotaxic space. Brain Struct Funct 212(6):481-95.

Catani M, ffytche DH. (2005): The rises and falls of disconnection syndromes. Brain 128(Pt 10):2224-39.

Catani M, Howard RJ, Pajevic S, Jones DK. (2002): Virtual in vivo interactive dissection of white matter fasciculi in the human brain. Neuroimage 17(1):77-94.

Catani, M., D. K. Jones, et al. (2005): Perisylvian language networks of the human brain. Ann Neurol 57(1): 8-16.

Cavada C, Goldman-Rakic PS. (1989): Posterior parietal cortex in rhesus monkey: II. Evidence for segregated corticocortical networks linking sensory and limbic areas with the frontal lobe. J Comp Neurol 287(4):422-45.

Corbetta M, Shulman GL. (2002): Control of goal-directed and stimulus-driven attention in the brain. Nat Rev Neurosci 3(3):201-15.

Duffau, H., P. Gatignol, et al. (2003): The articulatory loop: study of the subcortical connectivity by electrostimulation. Neuroreport 14(15): 2005-2008.

Decety J, Perani D, Jeannerod M, Bettinardi V, Tadary B, Woods R, Mazziotta JC, Fazio F. (1994): Mapping motor representations with positron emission tomography. Nature 371(6498):600-2.

Dehaene S, Spelke E, Pinel P, Stanescu R, Tsivkin S. (1999): Sources of mathematical thinking: behavioral and brain-imaging evidence. Science 284(5416):970-4.

Doricchi F, Thiebaut de Schotten M, Tomaiuolo F, Bartolomeo P. (2008): White matter (dis)connections and gray matter (dys)functions in visual neglect: gaining insights into the brain networks of spatial awareness. Cortex 44(8):983-95.

Doricchi F, Tomaiuolo F. (2003): The anatomy of neglect without hemianopia: a key role for parietal-frontal disconnection? Neuroreport 14(17):2239-43.

Eickhoff SB, Amunts K, Mohlberg H, Zilles K. (2006a): The human parietal operculum. II. Stereotaxic maps and correlation with functional imaging results. Cereb Cortex 16(2):268-79.

Eickhoff SB, Heim S, Zilles K, Amunts K. (2006b): Testing anatomically specified hypotheses in functional imaging using cytoarchitectonic maps. Neuroimage 32(2):570-82.

Eidelberg D, Galaburda AM. (1984): Inferior parietal lobule. Divergent architectonic asymmetries in the human brain. Arch Neurol 41(8):843-52.

Faglioni P, Basso A. (1985): Historical perspectives on neuroanatomical

correlates of limb apraxia. In: Roy E, editor. Neuropsychological studies of apraxia and related disorders. Amsterdam: North-Holland. p 3-44.

Fang PC, Stepniewska I, Kaas JH. (2005): Ipsilateral cortical connections of motor, premotor, frontal eye, and posterior parietal fields in a prosimian primate, Otolemur garnetti. J Comp Neurol 490(3):305-33.

Freund HJ. (2001): The parietal lobe as a sensorimotor interface: a perspective from clinical and neuroimaging data. Neuroimage 14(1 Pt 2):S142-6.

Fridman EA, Immisch I, Hanakawa T, Bohlhalter S, Waldvogel D, Kansaku K, Wheaton L, Wu T, Hallett M. (2006): The role of the dorsal stream for gesture production. Neuroimage 29(2):417-28.

Geschwind N. (1965a): Disconnexion syndromes in animals and man. I. Brain 88(2):237-94.

Geschwind N. (1965b): Disconnexion syndromes in animals and man. II. Brain 88(3):585-644.

Geschwind N, Damasio A. (1985): Apraxia. In: Vinken P, Bruyn G, Klawans H, editors. Handbook of clinical neurology. Amsterdam: Elsevier. p 423-32.

Geyer S, Matelli M, Luppino G, Zilles K. (2000): Functional neuroanatomy of the primate isocortical motor system. Anat Embryol (Berl) 202(6):443-74.

Goldring S, Harding GW, Gregorie EM. (1994): Distinctive electrophysiological characteristics of functionally discrete brain areas: a tenable approach to functional localization. J Neurosurg 80(4):701-9.

Goodale MA, Milner AD. (1992): Separate visual pathways for perception and action. Trends Neurosci 15(1):20-5.

Grafton ST, Fagg AH, Woods RP, Arbib MA. (1996): Functional anatomy of

pointing and grasping in humans. Cereb Cortex 6(2):226-37.

Grefkes C, Fink GR. (2005): The functional organization of the intraparietal sulcus in humans and monkeys. J Anat 207(1):3-17.

Grol MJ, de Lange FP, Verstraten FA, Passingham RE, Toni I. (2006): Cerebral changes during performance of overlearned arbitrary visuomotor associations. J Neurosci 26(1):117-25.

Haaland KY, Harrington DL, Knight RT. (2000): Neural representations of skilled movement. Brain 123 (Pt 11):2306-13.

Halsband U, Schmitt J, Weyers M, Binkofski F, Grutzner G, Freund HJ. (2001): Recognition and imitation of pantomimed motor acts after unilateral parietal and premotor lesions: a perspective on apraxia. Neuropsychologia 39(2):200-16.

Hattori N, Shibasaki H, Wheaton L, Wu T, Matsuhashi M, Hallett M. (2009): Discrete parieto-frontal functional connectivity related to grasping. J Neurophysiol 101(3):1267-82.

He BJ, Snyder AZ, Vincent JL, Epstein A, Shulman GL, Corbetta M. (2007): Breakdown of functional connectivity in frontoparietal networks underlies behavioral deficits in spatial neglect. Neuron 53(6):905-18.

Heilman KM, Rothi LJG. (2003): Apraxia. In: Heilman KM, Valenstein E, editors. Clinical Neuropsychology (4 ed.). New York: Oxford University Press. p 215-35.

Ikeda A, Hirasawa K, Kinoshita M, Hitomi T, Matsumoto R, Mitsueda T, Taki JY, Inouch M, Mikuni N, Hori T, Fukuyama H, Hashimoto N, Shibasaki H, Takahashi R. (2009): Negative motor seizure arising from the negative

motor area: is it ictal apraxia? Epilepsia 50(9):2072-84.

Ikeda A, Sato T, Ohara S, Matsuhashi M, Yamamoto J, Takayama M, Matsumoto R, Mikuni N, Takahashi J, Miyamoto S, Taki W, Hashimoto N, Shibasaki H. (2002): "Supplementary motor area (SMA) seizure" rather than "SMA epilepsy" in optimal surgical candidates: a document of subdural mapping. J Neurol Sci 202(1-2):43-52.

Jerva M, Holmes T, Goldring S, O'Leary J. (1960): Comparison of nembutal and procaine effects on direct cortical response in isolated cat cortex [abstract]. Fed Proc 19:291.

Johnson PB, Ferraina S, Bianchi L, Caminiti R. (1996): Cortical networks for visual reaching: physiological and anatomical organization of frontal and parietal lobe arm regions. Cereb Cortex 6(2):102-19.

Johnson-Frey SH, Newman-Norlund R, Grafton ST. (2005): A distributed left hemisphere network active during planning of everyday tool use skills. Cereb Cortex 15(6):681-95.

Karnath HO, Perenin MT. (2005): Cortical control of visually guided reaching: evidence from patients with optic ataxia. Cereb Cortex 15(10):1561-9.

Kleist K. (1931): Gehirnpathologische und lokalisatorische Ergenbnisse: das Stirnhirn im engeren Sinne und seine Storungen. Z ges Neurol Psychiat 131:442-8.

Lacruz ME, Garcia Seoane JJ, Valentin A, Selway R, Alarcon G. (2007): Frontal and temporal functional connections of the living human brain. Eur J Neurosci 26(5):1357-70.

Leiguarda RC, Marsden CD. (2000): Limb apraxias: higher-order disorders of

sensorimotor integration. Brain 123 (Pt 5):860-79.

Lewis JW, Van Essen DC. (2000): Corticocortical connections of visual, sensorimotor, and multimodal processing areas in the parietal lobe of the macaque monkey. J Comp Neurol 428(1):112-37.

Li C, Chou S. (1962): Cortical intracellular synaptic potentials and direct cortical stimulation. J Cell Comp Physiol 60:1-16.

Liepmann H. (1920): Apraxie. In: Brugsh H, editor. Ergebnisse der gesamten Medizin. Wien Berlin: Urban&Schwarzenberg. p 516-543.

Lüders H, Lesser R, Dinner D, Morris H, Hahn J, Friedman L, others. (1987): Commentary: chronic intracranial recording and stimulation with subdural electrodes. In: Engel JJ, editor. Surgical treatment of the epilepsies. New York: Raven Press. p 297-321.

Luppino G, Murata A, Govoni P, Matelli M. (1999): Largely segregated parietofrontal connections linking rostral intraparietal cortex (areas AIP and VIP) and the ventral premotor cortex (areas F5 and F4). Exp Brain Res 128(1-2):181-7.

Luria A. (1980): Higher cortical functions in man. 2nd ed. New York: Basic Books.

Makris N, Kennedy DN, McInerney S, Sorensen AG, Wang R, Caviness VS, Jr., Pandya DN. (2005): Segmentation of subcomponents within the superior longitudinal fascicle in humans: a quantitative, in vivo, DT-MRI study. Cereb Cortex 15(6):854-69.

Marusic P, Najm IM, Ying Z, Prayson R, Rona S, Nair D, Hadar E, Kotagal P, Bej MD, Wyllie E, Bingaman W, Lüders H. (2002): Focal cortical dysplasias in

eloquent cortex: functional characteristics and correlation with MRI and histopathologic changes. Epilepsia 43(1):27-32.

Matelli M, Camarda R, Glickstein M, Rizzolatti G. (1986): Afferent and efferent projections of the inferior area 6 in the macaque monkey. J Comp Neurol 251(3):281-98.

Matelli M, Govoni P, Galletti C, Kutz DF, Luppino G. (1998): Superior area 6 afferents from the superior parietal lobule in the macaque monkey. J Comp Neurol 402(3):327-52.

Matsuhashi M, Ikeda A, Ohara S, Matsumoto R, Yamamoto J, Takayama M, Satow T, Begum T, Usui K, Nagamine T, Mikuni N, Takahashi J, Miyamoto S, Fukuyama H, Shibasaki H. (2004): Multisensory convergence at human temporo-parietal junction - epicortical recording of evoked responses. Clin Neurophysiol 115(5):1145-60.

Matsumoto R, Ikeda A, Ohara S, Matsuhashi M, Baba K, Yamane F, Hori T, Mihara T, Nagamine T, Shibasaki H. (2003): Motor-related functional subdivisions of human lateral premotor cortex: epicortical recording in conditional visuomotor task. Clin Neurophysiol 114(6):1102-15.

Matsumoto R, Imamura H, Inouch M, Nakagawa T, Yokoyama Y, Matsuhashi M, Mikuni N, Miyamoto S, Fukuyama H, Takahashi R, Ikeda A. (2011): Left anterior temporal cortex actively engages in speech perception: A direct cortical stimulation study. Neuropsychologia 49 (5): 1350-4.

Matsumoto R, Nair D. (2007): Cortico-cortical evoked potentials to define eloquent cortex. In: Lüders H, editor. Textbook of epilepsy surgery. Abington: Taylor&Francis Books Ltd. p 1049-59.

Matsumoto R, Nair DR, LaPresto E, Bingaman W, Shibasaki H, Lüders HO. (2007a): Functional connectivity in human cortical motor system: a cortico-cortical evoked potential study. Brain 130(Pt 1):181-97.

Matsumoto R, Nair DR, LaPresto E, Najm I, Bingaman W, Lüders HO. (2004a): Cortico-cortical evoked potentials. In: Lüders HO, editor. Deep brain stimulation and epilepsy. London: Martin Dunitz. p 105-111.

Matsumoto R, Nair DR, LaPresto E, Najm I, Bingaman W, Shibasaki H, Lüders HO. (2004b): Functional connectivity in the human language system: a cortico-cortical evoked potential study. Brain 127(Pt 10):2316-30.

Matsumoto R, Sawamoto N, Taki J, Mitsueda T, Inouchi M, Hitomi T, Kinoshita M, Urayama S, Mikuni N, Behrens T, Fukuyama H, Takahashi R, Ikeda A. (2007b): Cortico-cortical network involved in secondary epileptogenesis: a combined study of functional and anatomical tractography. Epilepsia 48(suppl 7):44 [abstract].

Mesulam M. (2000): Principles of behavioral and cognitive neurology. Oxford: Oxford university press.

Mesulam M. (2005): Imaging connectivity in the human cerebral cortex: the next frontier? Ann Neurol 57(1):5-7.

Papagno C, Della Sala S, Basso A. (1993): Ideomotor apraxia without aphasia and aphasia without apraxia: the anatomical support for a double dissociation. J Neurol Neurosurg Psychiatry 56(3):286-9.

Perenin MT, Vighetto A. (1988): Optic ataxia: a specific disruption in visuomotor mechanisms. I. Different aspects of the deficit in reaching for objects. Brain 111 (Pt 3):643-74.

Petrides M, Pandya DN. (1984): Projections to the frontal cortex from the posterior parietal region in the rhesus monkey. J Comp Neurol 228(1):105-16.

Picard N, Strick PL. (2001): Imaging the premotor areas. Curr Opin Neurobiol 11(6):663-72.

Prado J, Clavagnier S, Otzenberger H, Scheiber C, Kennedy H, Perenin MT. (2005): Two cortical systems for reaching in central and peripheral vision. Neuron 48(5):849-58.

Raymer AM, Merians AS, Adair JC, Schwartz RL, Williamson DJ, Rothi LJ, Poizner H, Heilman KM. (1999): Crossed apraxia: implications for handedness. Cortex 35(2):183-99.

Rizzolatti G, Luppino G, Matelli M. (1998): The organization of the cortical motor system: new concepts. Electroencephalogr Clin Neurophysiol 106(4):283-96.

Rosenberg DS, Mauguiere F, Catenoix H, Faillenot I, Magnin M. (2009): Reciprocal thalamocortical connectivity of the medial pulvinar: a depth stimulation and evoked potential study in human brain. Cereb Cortex 19(6):1462-73.

Rozzi S, Calzavara R, Belmalih A, Borra E, Gregoriou GG, Matelli M, Luppino G. (2006): Cortical connections of the inferior parietal cortical convexity of the macaque monkey. Cereb Cortex 16(10):1389-417.

Rushworth MF, Behrens TE, Johansen-Berg H. (2006): Connection patterns distinguish 3 regions of human parietal cortex. Cereb Cortex 16(10):1418-30.

Scheperjans F, Eickhoff SB, Homke L, Mohlberg H, Hermann K, Amunts K, Zilles K. (2008): Probabilistic maps, morphometry, and variability of cytoarchitectonic areas in the human superior parietal cortex. Cereb Cortex 18(9):2141-57.

Schmahmann J, Pandya D. (2006): Superior longitudinal fasciculus and arcuate fasciculus. In: Schmahmann J, Pandya D, editors. Fiber pathways of the brain. Oxford: Oxford university press. p 393-408.

Simon O, Kherif F, Flandin G, Poline JB, Riviere D, Mangin JF, Le Bihan D, Dehaene S. (2004): Automatized clustering and functional geometry of human parietofrontal networks for language, space, and number. Neuroimage 23(3):1192-202.

Simon O, Mangin JF, Cohen L, Le Bihan D, Dehaene S. (2002): Topographical layout of hand, eye, calculation, and language-related areas in the human parietal lobe. Neuron 33(3):475-87.

Stepniewska I, Preuss TM, Kaas JH. (2006): Ipsilateral cortical connections of dorsal and ventral premotor areas in New World owl monkeys. J Comp Neurol 495(6):691-708.

Tanne J, Boussaoud D, Boyer-Zeller N, Rouiller EM. (1995): Direct visual pathways for reaching movements in the macaque monkey. Neuroreport 7(1):267-72.

Thiebaut de Schotten M, Urbanski M, Duffau H, Volle E, Levy R, Dubois B, Bartolomeo P. (2005): Direct evidence for a parietal-frontal pathway subserving spatial awareness in humans. Science 309(5744):2226-8.

Thiebaut de Schotten M, Dell'Acqua F, Forkel S, Simmons A, Vergani F, Murphy

DGM, Catani M. A Lateralized Brain Network for Visuo-Spatial Attention. (2011): Nature Precedings <http://hdl.handle.net/10101/npre.2011.5549.1>

Tomassini V, Jbabdi S, Klein JC, Behrens TE, Pozzilli C, Matthews PM, Rushworth MF, Johansen-Berg H. (2007): Diffusion-weighted imaging tractography-based parcellation of the human lateral premotor cortex identifies dorsal and ventral subregions with anatomical and functional specializations. J Neurosci 27(38):10259-69.

Van Essen DC. (1997): A tension-based theory of morphogenesis and compact wiring in the central nervous system. Nature 385(6614):313-8.

Van Essen DC, Lewis JW, Drury HA, Hadjikhani N, Tootell RB, Bakircioglu M, Miller MI. (2001): Mapping visual cortex in monkeys and humans using surface-based atlases. Vision Res 41(10-11):1359-78.

Vigneau M, Beaucousin V, Herve PY, Duffau H, Crivello F, Houde O, Mazoyer B, Tzourio-Mazoyer N. (2006): Meta-analyzing left hemisphere language areas: phonology, semantics, and sentence processing. Neuroimage 30(4):1414-32.

Wakana S, Jiang H, Nagae-Poetscher LM, van Zijl PC, Mori S. (2004): Fiber tract-based atlas of human white matter anatomy. Radiology 230(1):77-87.

Weinrich M, Wise SP, Mauritz KH. (1984): A neurophysiological study of the premotor cortex in the rhesus monkey. Brain 107 (Pt 2):385-414.

Wheaton LA, Hallett M. (2007): Ideomotor apraxia: a review. J Neurol Sci 260(1-2):1-10.

Wheaton LA, Nolte G, Bohlhalter S, Fridman E, Hallett M. (2005): Synchronization of parietal and premotor areas during preparation and execution of praxis hand movements. Clin Neurophysiol 116(6):1382-90.

Wise SP, Boussaoud D, Johnson PB, Caminiti R. (1997): Premotor and parietal cortex: corticocortical connectivity and combinatorial computations. Annu Rev Neurosci 20:25-42.

Yamamoto H, Fukunaga M, Takahashi S, Mano H, Tanaka C, Umeda M, Ejima Y. (2011): Inconsistency and uncertainty of the human visual area loci following surface-based registration: probability and entropy maps Human Brain Mapp. 32: n/a. doi: 10.1002/hbm.21200

Figure legends

Figure 1

Schematic diagram illustrating the coordinates for displaying the sites of stimulation and maximum CCEP response in the lateral parietal and frontal area.

(A) Distances from the central sulcus along the rostro-caudal dimension are plotted for the parietal stimulus sites in the abscissa and for the frontal recording sites in the ordinate. The distance from the central sulcus was measured on a line drawn parallel to the AC-PC line.

(B) Along the dorso-ventral dimension, the parietal stimulus sites were measured from the intraparietal sulcus (IPS, dotted line) and the frontal recording sites were measured from the border between the dorsal and ventral premotor areas (broken line).

CS = central sulcus; IFS = inferior frontal sulcus; IPS = intraparietal sulcus; PrCS = precentral sulcus; PMd = dorsal premotor area; PMv = ventral premotor area; SFS = superior frontal sulcus

Figure 2

CCEPs recorded from the lateral premotor area in a representative case (Patient 1). CCEPs are plotted with subaverages (black and grey waveforms) in reference to the major sulci identified on 3D MRI (left lower corner of each figure). The vertical line corresponds to the time of single pulse stimulation. On 3D MRI, each parietal stimulus site is shown as a pair of interconnected black electrodes and the whole area covered by the recording electrodes is

shaded white. Maximum response of the main CCEP field is plotted as a white circle, while that of smaller, separate CCEP fields, if present, as a black circle. CCEPs elicited by parietal stimulation of the same dorso-ventral division are displayed in the same row (A-C and D-F, respectively). Note that the more caudal the parietal stimulus site is located, the more rostral the frontal maximum response site is located (i.e., more distant from CS). Other conventions are the same as for Fig. 1 except for Sylv = Sylvian fissure.

Figure 3

Spatial relationship between the sites of stimulation and maximum CCEP response in the rostro-caudal coordinate (A) and in the dorso-ventral coordinate (B). In (A), the distance of the parietal stimulus sites (abscissa) and of the frontal response sites (ordinate) was measured from the central sulcus. In (B), the distance of the parietal stimulus sites (abscissa) was measured from the intraparietal sulcus (IPS) that is the border between SPL and IPL, and that of the frontal response sites (ordinate) was measured from the border between PMv and PMd (see text for more details). In terms of the distance from the stimulus and response sites, regression analysis showed a positive correlation between the sites of stimulation and maximum response both for the rostrocaudal (A) and dorsoventral (B) axes. Consistent with the mirror-symmetric configuration across the central sulcus as shown in (A), a positive correlation was observed between the surface distance from the parietal stimulus sites to the frontal response sites and the N1 peak latency of the maximum response (C). Conventions are the same as for Fig. 1.

Figure 4

Representative CCEP distribution indicative of multiple parieto-frontal connections in Patient 2 (left) and 3 (right). Besides the predominant parieto-frontal connection as judged by the prominent CCEP field (maximum response shown in white circle), additional connections were identified based on spatially separate fields (maximum response in black circle). Three separate connections were traced from the supramarginal gyrus to the ventral premotor area in Patient 2, while in Patient 3 stimulation of the postcentral gyrus revealed two separate connections to the adjacent precentral gyrus and ventral premotor area. Implanted hemispheres are shown on the same side for the sake of presentation by flipping the sides (Patient 2). See Fig. 2 also for multiple connections in Patient 1. Conventions are the same as for Fig. 2.

Figure 5

Functional connections from the ventral parietal area to the premotor area revealed in the vicinity of astrocytoma (shadowed) located in the precentral gyrus in Patient 5. Stimulation at the supramarginal gyrus elicited CCEP ventral to the tumor at around the ventral ramus of the precentral sulcus. CCEP was not observed rostral to the tumor. Note the network configuration was similar to that seen in an epilepsy patient (e.g., Fig. 2E), in whom epileptic foci were away from the area of investigation. Conventions are the same as for Fig. 2.

Figure 6

3D display of the stimulus and response sites in the MNI standard space. The stimulus and response sites are accumulated from all the patients and coregistered into the MNI standard space. All the stimulus and response sites are collapsed onto the left convexity for a display purpose. Stimulus sites are labeled and displayed together according to the Jülich cytoarchitectonic atlas on the same 3D brain (see the label in the left upper corner of each 3D brain). Regarding the frontal CCEP responses, a large sphere represents the location of the electrode showing the maximum CCEP response, i.e., the target site of the predominant connection from the stimulus site. A small sphere represents the electrode showing the maximum response of the additional, separate CCEP field, i.e., the target site of the additional divergent connection from the stimulus site. Note the location of the maximum and additional response sites may be overlapped within the lateral frontal area. Also note that the parieto-frontal connections were not equally distributed along the central sulcus partly due to the less electrode coverage in the dorsal part than the ventral part. The lateral view of the 3D brain in the right lower corner indicates the parietal segmentations of the Jülich atlas where electrical stimuli were applied.

Table 1 Patient profile

Patient	1	2	3	4	5	6	7
Age, gender, handedness	33M R	37F R	39M R	54M R	17M R	32F R	23F R
Etiology	MTLE	MTLE	partial epilepsy*	astrocytoma	DNT	FCD Type IA	FCD Type IA
Implanted hemisphere	R	L	R	L	R	L	R
Number of electrode pairs stimulated on the parietal cortex	14	11	12	4	4	10	9
Number of recording electrodes placed on the frontal cortex	15	23	22	19	13	11	17
Neurological examination	normal	normal	normal	mild R hand weakness & dysarthria	normal	normal	normal

MTLE = mesial temporal lobe epilepsy; DNT = dysembryoplastic neuroepithelial tumor; FCD = focal cortical dysplasia

* epileptic focus was non-localizable

Table 2

Summary of the parietal stimulus and frontal response sites in reference to the Jülich cytoarchitectonic atlas in the MNI standard space

FRONTAL RESPONSE SITE

PARIETAL STIMULUS SITE	BA6dc	BA6vc	BA6dr	BA44	BA45	subtotal
BA1v	-/-	**3**/2	-/-	-/1	-/1	**3**/4
BA2v	-/-	**1**/1	-/-	-/1	**1**/1	**2**/3
OP4	-/1	**2**/-	-/-	**1**/3	-/-	**3**/4
PFop	-/-	-/-	-/-	**1**/-	-/-	**1**/-
PFt	-/-	**1**/-	-/-	-/1	-/-	**1**/1
PF	**1**/2	**1**/8	**1**/1	**6**/2	**3**/2	**12**/15
PFm	-/-	-/-	**3**/3	**4**/3	-/3	**7**/9
PGa	-/-	**1**/-	**2**/-	-/1	-/-	**3**/1
PGp	-/-	-/-	-/-	**3**/-	-/-	**3**/-
BA1d	**9**/-	-/1	**1**/2	-/1	-/-	**10**/4
BA2d	**2**/1	-/-	-/-	-/1	-/-	**2**/2
7PC	**1**/-	**1**/-	-/-	-/-	-/-	**2**/-
7A	-/-	-/-	**2**/-	**1**/-	-/-	**3**/-
subtotal	**13**/4	**10**/12	**9**/6	**16**/14	**4**/7	total **52**/43

Number of the maximum (left, bold) and additional (right) responses is shown in each cell, -: no response
See definitions of BA1v, BA1d, BA2d, BA2v, BA6dr, BA6dc, BA6vc in the text.

Table 3

Individual cytoarchitectonic labels and MNI coordinates of the stimulus and response sites

	Parietal stimulus site				Target site of the predominant connection				Target sites of additional connections											
Subject	Label	MNI coordinate (x,y,z)			Label	MNI coordinate			Label	MNI coordinate			Label	MNI coordinate			Label	MNI coordinate		
Patient 1	BA1d	52	-22	58	BA6dr	30	-2	64												
Patient 1	BA1d	36	-38	70	BA6dc	34	-26	72												
Patient 3	BA1d	30	-43	75	BA6dc	26	-14	76												
Patient 3	BA1d	48	-34	62	BA6dc	34	-14	70	BA6vc	60	6	36								
Patient 3	BA1d	30	-33	73	BA6dc	36	-24	72												
Patient 3	BA1d	50	-24	62	BA6dc	44	-14	66	BA6vc	60	6	36								
Patient 4	BA1d	-53	-21	57	BA6dc	-44	-10	57												
Patient 5	BA1d	23	-34	77	BA6dc	28	-24	74	BA6dr	30	-4	70								
Patient 5	BA1d	35	-37	70	BA6dc	28	-24	74	BA6dr	20	-4	74								
Patient 6	BA1d	-53	-19	54	BA6dc	-49	-6	54	BA44	-62	10	12								
Patient 6	BA1v	-64	-7	27	BA6vc	-63	0	16	BA44	-62	10	12								
Patient 7	BA1v	65	-5	33	BA6vc	61	2	35	BA45	58	36	2	BA6vc	58	14	34				
Patient 7	BA1v	60	-10	43	BA6vc	61	2	35	BA6vc	58	14	34								
Patient 1	BA2d	31	-47	70	BA6dc	34	-26	72												
Patient 6	BA2d	-52	-33	55	BA6dc	-49	-6	54	BA44	-62	10	12	BA6dc	-48	4	49				
Patient 1	BA2v	60	-21	48	BA6vc	56	-8	48	BA44	60	18	20								
Patient 7	BA2v	61	-22	47	BA45	62	20	22	BA45	58	36	2	BA6vc	61	2	35				
Patient 1	OP4	67	-7	25	BA6vc	60	8	34	BA44	60	18	20								
Patient 6	OP4	-65	-16	30	BA6vc	-62	4	27	BA44	-62	10	12	BA44	-49	12	47	BA6dc	-49	-6	54
Patient 7	OP4	69	-7	17	BA44	62	16	12												
Patient 1	PF	67	-30	33	BA44	60	18	20	BA6vc	58	0	46								
Patient 4	PF	-64	-32	37	BA44	-58	14	22												
Patient 6	PF	-61	-39	40	BA44	-62	10	12	BA6vc	-58	10	38	BA6dc	-49	-6	54				
Patient 6	PF	-64	-28	38	BA44	-62	10	12	BA6dc	-49	-6	54	BA6vc	-62	4	27				
Patient 7	PF	68	-30	24	BA44	62	16	12												
Patient 7	PF	68	-23	29	BA44	62	16	12	BA45	58	36	2	BA6vc	61	2	35				
Patient 2	PF	-63	-48	29	BA45	-49	34	22	BA44	-58	16	5								
Patient 7	PF	68	-37	18	BA45	58	30	16												
Patient 7	PF	60	-34	48	BA45	62	20	22	BA45	56	30	-8								
Patient 1	PF	65	-40	35	BA6dr	46	3	54	BA6vc	58	0	46								
Patient 1	PF	57	-32	52	BA6dc	45	-18	62	BA44	60	18	20	BA6dr	48	14	52				
Patient 6	PF	-47	-45	57	BA6vc	-58	10	38	BA6vc	-63	0	16	BA6vc	-58	2	41				

Patient 1	PFm	53	-44	55	BA44	60	18	20	BA6dr	48	14	52	BA6dr	30	-2	64	
Patient 2	PFm	-59	-57	33	BA44	-49	18	44	BA44	-58	16	5	BA45	-49	34	22	
Patient 6	PFm	-54	-59	44	BA44	-55	18	33									
Patient 6	PFm	-58	-49	42	BA44	-62	10	12	BA44	-55	18	33					
Patient 1	PFm	49	-52	54	BA6dr	30	-2	64	BA44	60	18	20	BA6dr	48	14	52	
Patient 1	PFm	61	-52	37	BA6dr	35	8	62									
Patient 2	PFm	-55	-53	43	BA6dr	-47	4	51	BA45	-53	26	-2	BA45	-46	34	32	
Patient 7	PFop	69	-18	22	BA44	62	16	12									
Patient 1	PFt	67	-19	30	BA6vc	60	8	34	BA44	60	18	20					
Patient 1	PGa	42	-63	55	BA6dr	30	-2	64	BA44	60	18	20					
Patient 3	PGa	44	-55	56	BA6dr	30	-2	67									
Patient 6	PGa	-41	-55	59	BA6vc	-58	10	38									
Patient 2	PGp	-42	-70	49	BA44	-55	16	37									
Patient 2	PGp	-45	-73	42	BA44	-49	18	44									
Patient 2	PGp	-49	-76	30	BA44	-49	18	44									
Patient 2	7A	-34	-69	57	BA44	-55	16	37									
Patient 1	7A	26	-56	70	BA6dr	30	-2	64									
Patient 5	7A	23	-53	74	BA6dr	20	-4	74									
Patient 3	7PC	45	-44	60	BA6dc	34	-14	70									
Patient 2	7PC	-42	-50	60	BA6vc	-62	4	32									

Figure 1

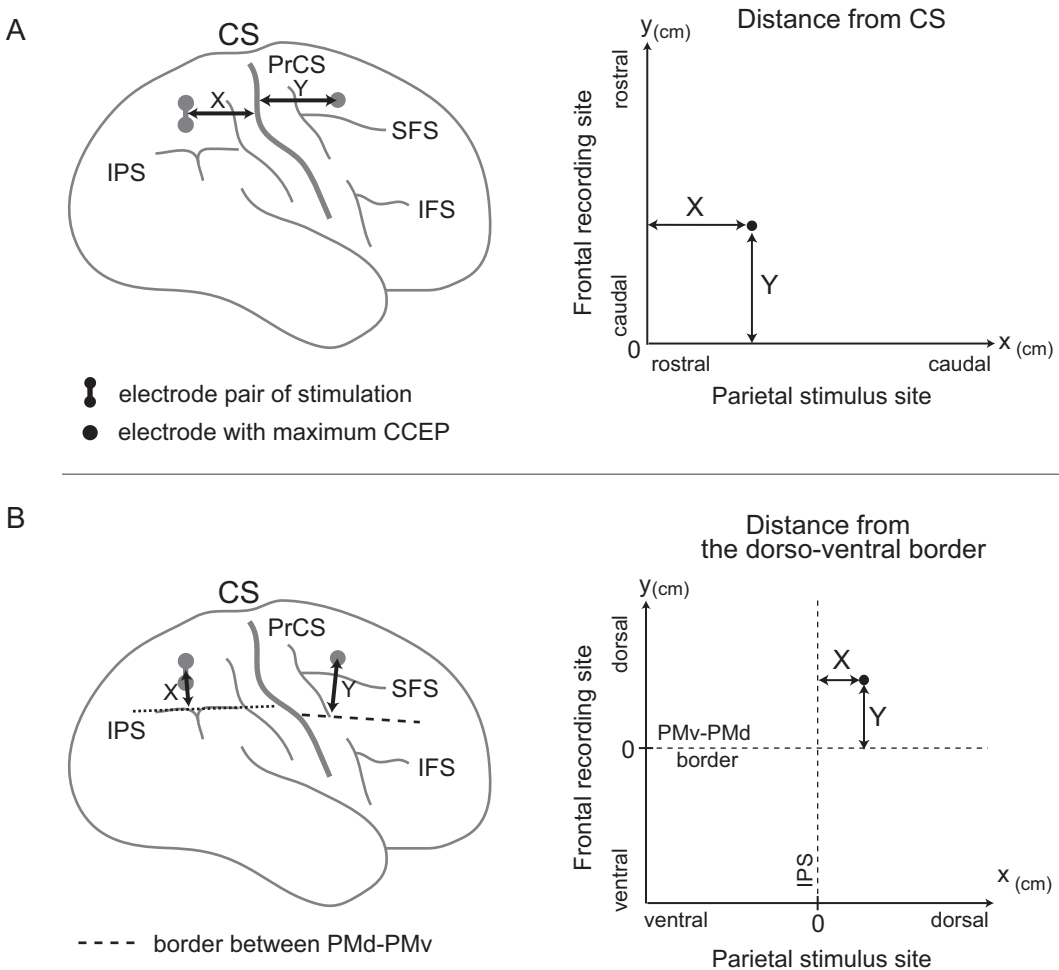
A
CS
PrCS
X
Y
SFS
IPS
IFS
electrode pair of stimulation
electrode with maximum CCEP
Distance from CS
y (cm)
rostral
caudal
Frontal recording site
X
Y
0
x (cm)
rostral
caudal
Parietal stimulus site
B
CS
PrCS
X
Y
SFS
IPS
IFS
border between PMd-PMv
Distance from
the dorso-ventral border
y (cm)
dorsal
ventral
Frontal recording site
X
Y
PMv-PMd
border
0
IPS
x (cm)
ventral
0
dorsal
Parietal stimulus site

Figure 2

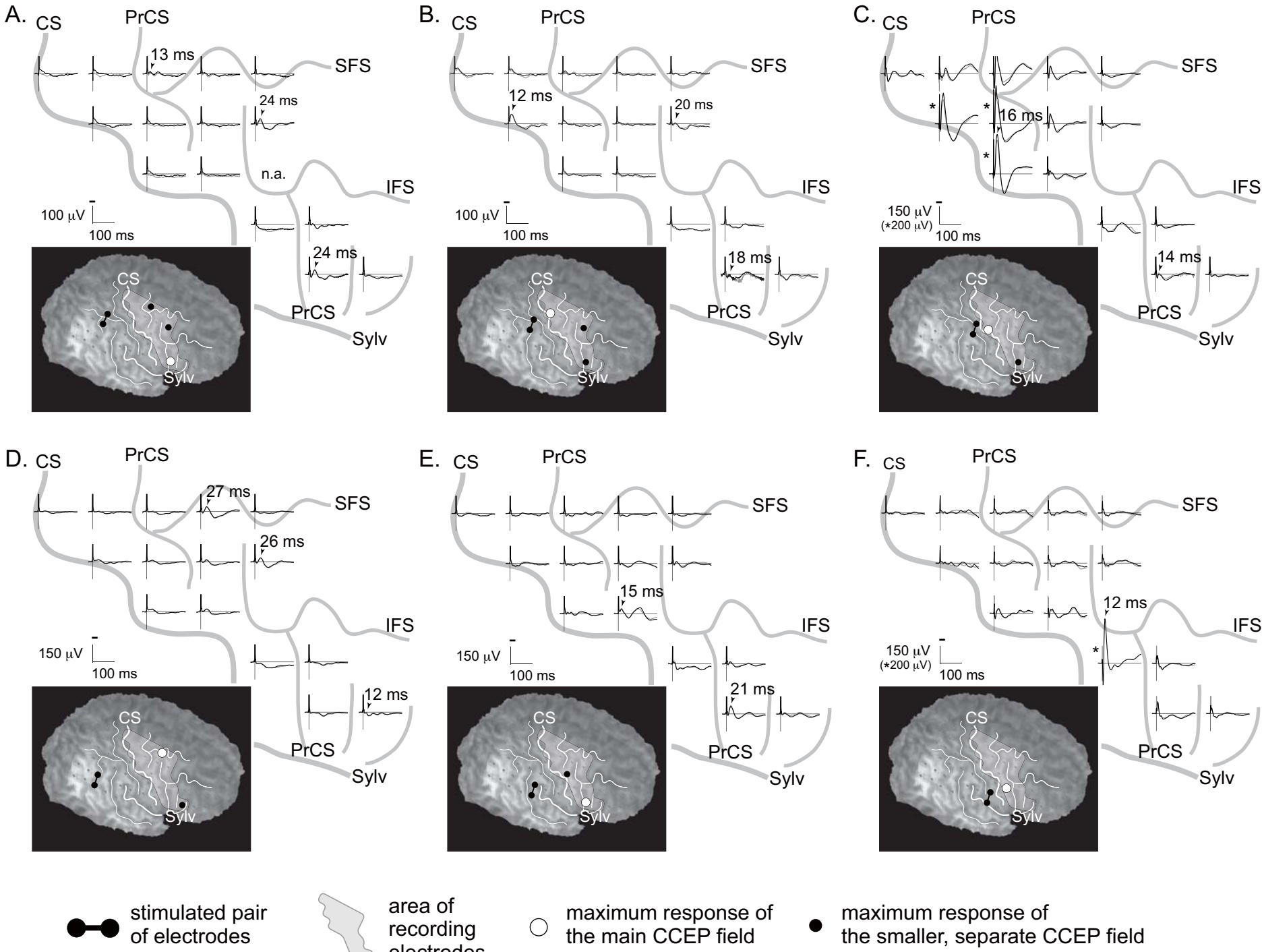
A.
CS
PrCS
13 ms
SFS
24 ms
n.a.
IFS
100 µV
100 ms
24 ms
CS
PrCS
Sylv
Sylv
B.
CS
PrCS
SFS
12 ms
20 ms
IFS
100 µV
100 ms
18 ms
CS
PrCS
Sylv
Sylv
C.
CS
PrCS
SFS
*
*
16 ms
*
IFS
150 µV
(*200 µV)
100 ms
14 ms
CS
PrCS
Sylv
Sylv
D.
CS
PrCS
27 ms
SFS
26 ms
IFS
150 µV
100 ms
12 ms
CS
PrCS
Sylv
Sylv
E.
CS
PrCS
SFS
15 ms
IFS
150 µV
100 ms
21 ms
CS
PrCS
Sylv
Sylv
F.
CS
PrCS
SFS
12 ms
IFS
150 µV
(*200 µV)
100 ms
*
CS
PrCS
Sylv
Sylv
stimulated pair of electrodes
area of recording electrodes
maximum response of the main CCEP field
maximum response of the smaller, separate CCEP field

Figure 3

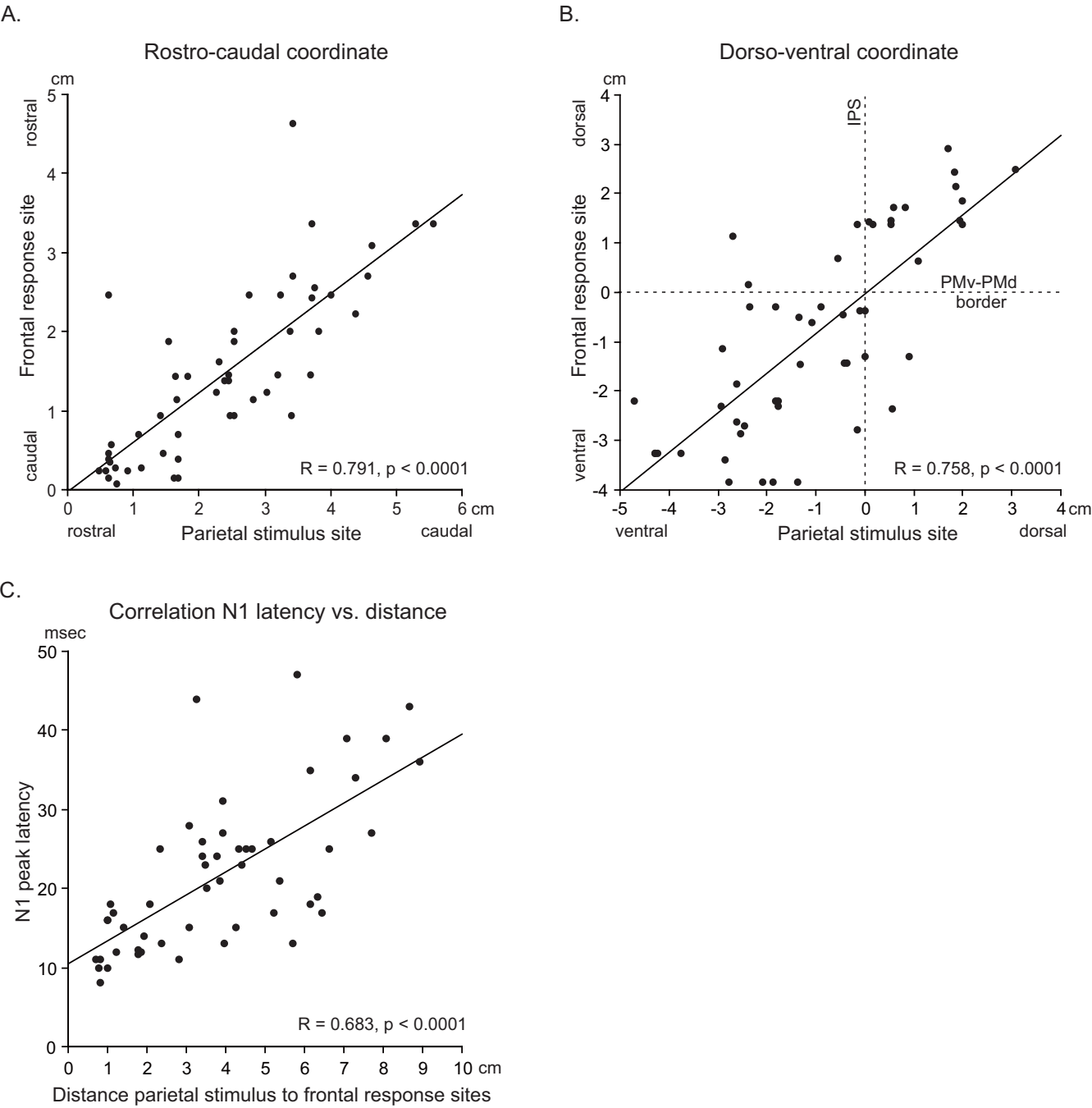
A.
Rostro-caudal coordinate
cm
rostral
caudal
Frontal response site
R = 0.791, p < 0.0001
rostral
Parietal stimulus site
caudal
B.
Dorso-ventral coordinate
cm
dorsal
ventral
IPS
PMv-PMd
border
Frontal response site
R = 0.758, p < 0.0001
ventral
Parietal stimulus site
dorsal
C.
Correlation N1 latency vs. distance
msec
N1 peak latency
R = 0.683, p < 0.0001
Distance parietal stimulus to frontal response sites

Figure 4

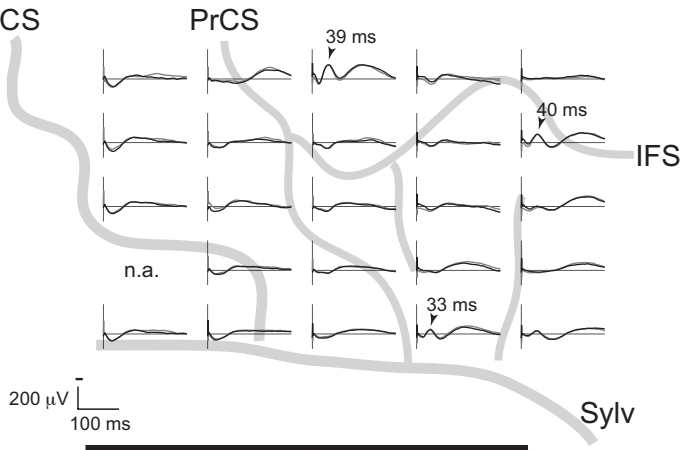
CS
PrCS
39 ms
40 ms
IFS
n.a.
33 ms
200 μV
100 ms
Sylv

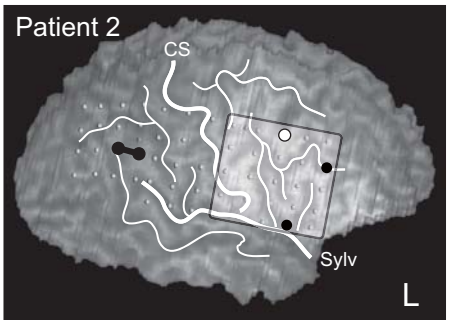
Patient 2
CS
Sylv
L

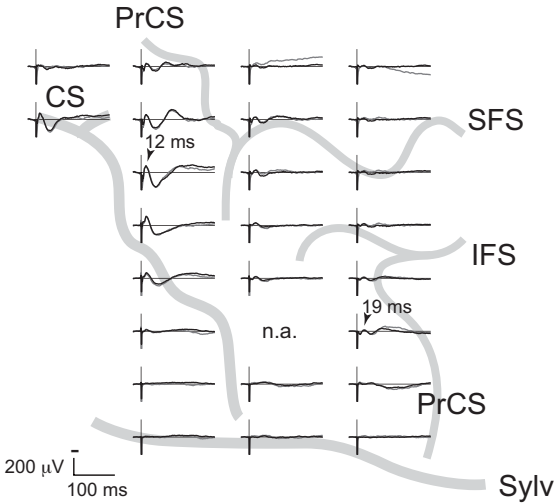
PrCS
CS
SFS
12 ms
IFS
19 ms
n.a.
PrCS
200 μV
100 ms
Sylv

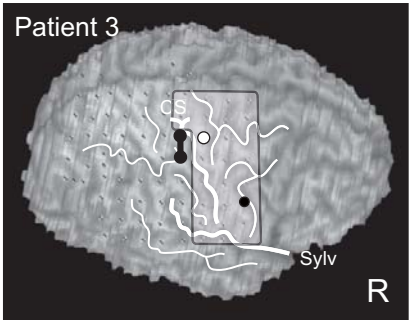
Patient 3
CS
Sylv
R

Figure 5

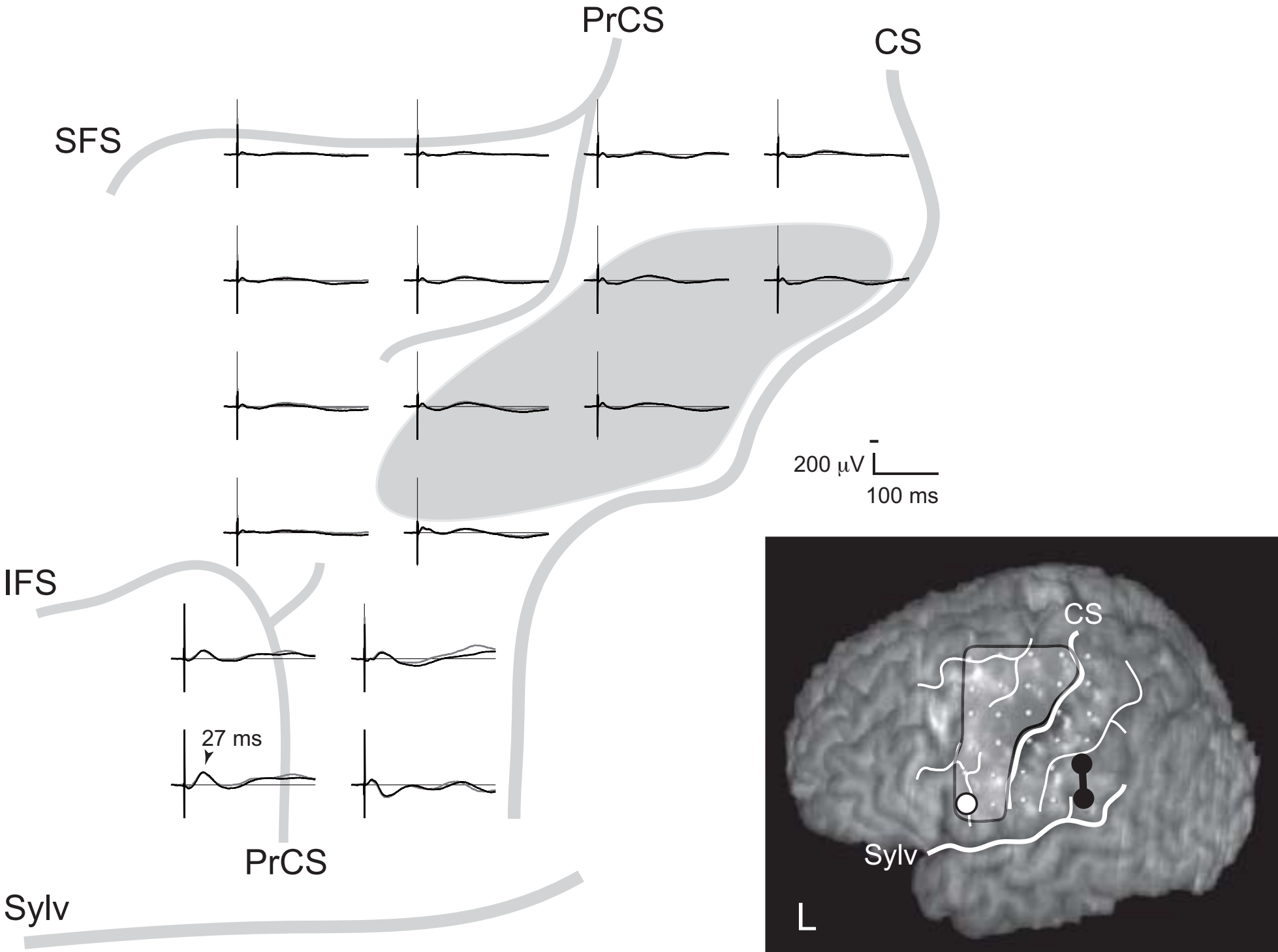

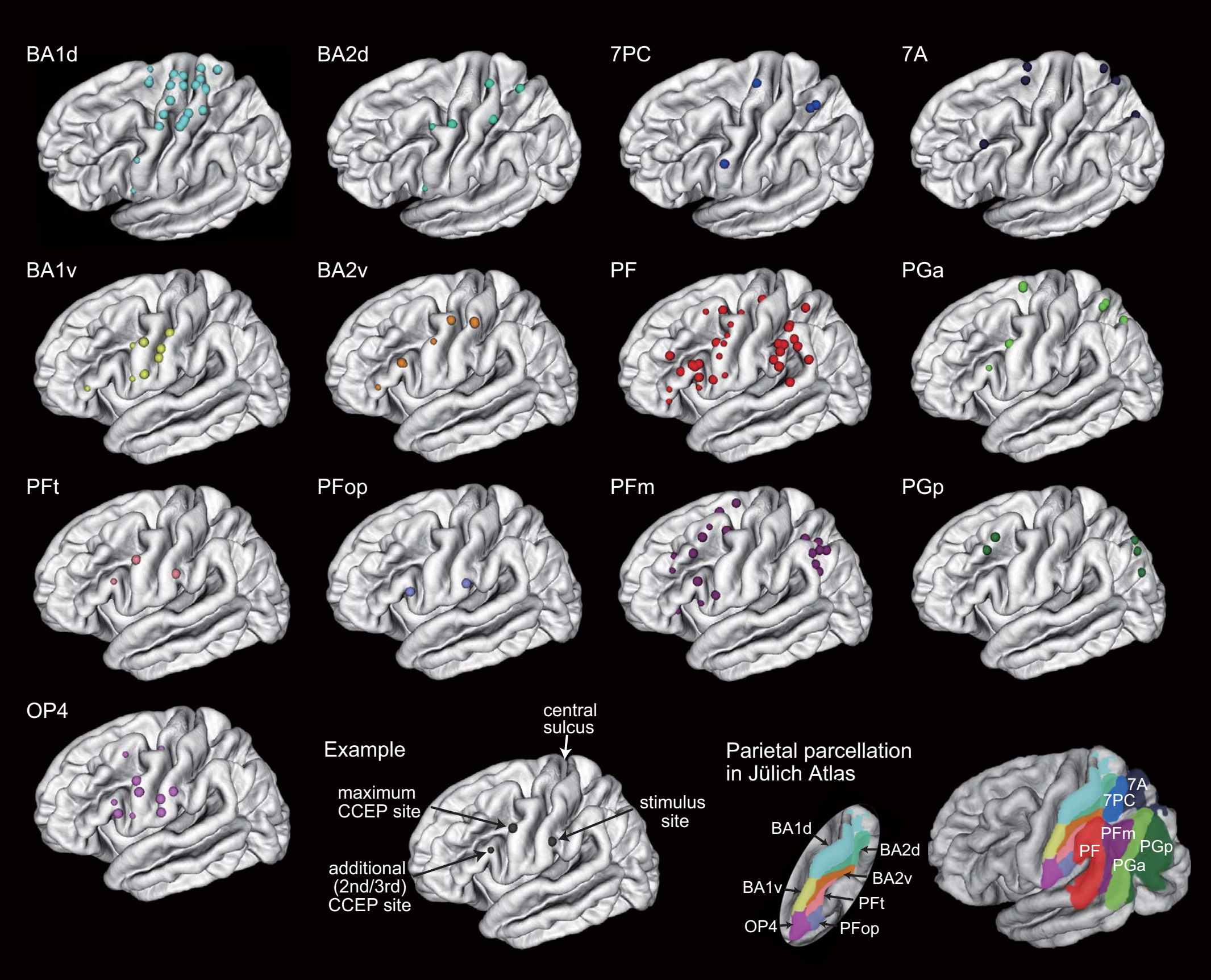
BA1d
BA2d
7PC
7A
BA1v
BA2v
PF
PGa
PFt
PFop
PFm
PGp
OP4
Example
central sulcus
maximum CCEP site
stimulus site
additional (2nd/3rd) CCEP site
Parietal parcellation in Jülich Atlas
BA1d
BA2d
BA2v
BA1v
PFt
OP4
PFop
7A
7PC
PFm
PF
PGp
PGa